

Magnetic, Structural, and Superconducting Properties of the Layered AFe_2As_2 Series of Compounds

Michael Nicklas, Alex Amato¹, Horst Borrmann, Ulrich Burkhardt, Nubia Caroca-Canales, Philipp Gegenwart², Michael Hanfland³, Andreas Hoser⁴, Zakir Hossain⁵, Hirale S. Jeevan², Anton Jesche, Koji Kaneko⁶, Deepa Kasinathan, Rustem Khasanov¹, Hans-Henning Klauss⁷, Katrin Koch, Cornelius Krellner, Manoj Kumar, Andreas Leithe-Jasper, Edit Lengyel, Hubertus Luetkens¹, Corneliu F. Miclea, Alim Ormeci, Helge Rosner, Miriam Schmitt, Walter Schnelle, Ulrich Schwarz, Oliver Stockert, and Christoph Geibel

Introduction

After the discovery of superconductivity at 26 K in the Fe-based system $LaFeAsO_{1-x}F_x$ ($x = 0.05 - 0.12$) [1] the physics community around the world has been tirelessly working for the past year to achieve an understanding of the intriguing properties of these compounds and to increase the superconducting transition temperature T_c . Spirited search by the experimentalists has eventually led to raising T_c to 55 K for another member of this $ROFeAs$ ($R =$ rare-earth element) family of compounds, $SmFeAsO_{0.9}F_{0.1}$ [2]. Shortly afterwards, the AFe_2As_2 ($A = Ca, Sr, Ba, Eu$) series of compounds was found to display very similar properties and to also become superconducting upon hole doping on the A site with a maximum T_c of 38 K [3,4,5]. These discoveries were followed by the announcements of further parent compounds: $LiFeAs$, $FeSe$, $SrFeAsF$ with a maximum T_c of 18 K [6], 14 K [6] (27 K using pressure [7]) and 56 K [8], respectively. The basic features common to these parent compounds are the antiferromagnetic (AF) ordering of the Fe spins at $T_N \approx 100-200$ K, and the layered nature of the electronic

structure. All the members belonging to the above mentioned families have been shown to superconduct upon either “hole” or “electron doping” or both. Superconductivity also emerges upon application of hydrostatic pressure for certain members of the $ROFeAs$, AFe_2As_2 and $FeSe$ families. Notwithstanding the abundant research that has already been performed, the microscopic nature of the superconducting pairing mechanism has thus far remained elusive.

We were among the first groups realizing the profound analogy between the $ROFeAs$ (1111) and the AFe_2As_2 (122) compounds and to start the synthesis and the investigation of the latter ones. Although the $ROFeAs$ systems have higher T_c values, the focus of the scientific community has shifted towards the 122 systems because the synthesis and the crystal growth of these compounds is easier and much better controllable than that of the 1111 compounds. Especially the adjustment of O and F content, which tunes the ground state from AF order of Fe moments to superconductivity, is rather difficult, in contrast to the substitution of (K, Na) for (Ca, Sr, Ba, or Eu) or of Co for Fe. Thus, while $RFeAsO$ single crystals are still in the sub-

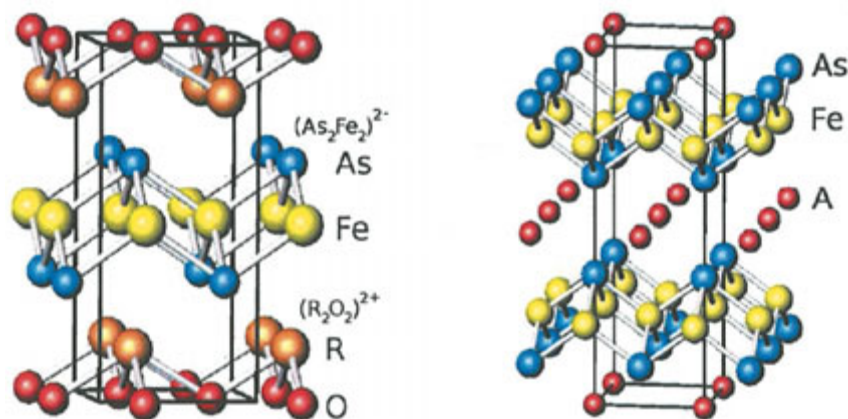


Fig. 1: Crystal structures of $RFeAsO$ (left, $ZrCuSiAs$ type) and AFe_2As_2 (right, $ThCr_2Si_2$ type).

millimeter range, 122 crystals have meanwhile reached surfaces $> 50 \text{ mm}^2$. The $A\text{Fe}_2\text{As}_2$ compounds crystallize in the tetragonal ThCr_2Si_2 -type crystal structure at room temperature. The FeAs layers in this structure are identical to the FeAs layer in the 1111 compounds, while the A atoms replace the RO layers in between. All the $A\text{Fe}_2\text{As}_2$ compounds with divalent A cation exhibit a structural transition upon cooling to an orthorhombic lattice (for Ca $T_0 \approx 171 \text{ K}$ [9], Sr $\approx 205 \text{ K}$ [10], Ba $\approx 140 \text{ K}$ [11], Eu $\approx 200 \text{ K}$ [12]). The structural transition is coupled with an antiferromagnetic ordering of the Fe moments with a wave vector $\mathbf{q} = [1,0,1]$ corresponding to a columnar arrangement of the Fe moments (see below). Suitable substitution on either the A site or the Fe site suppresses the magnetic ordering, and then the system becomes superconducting for certain ranges of doping. Superconductivity can also be induced in “undoped” and “under-doped” compounds by applying pressure.

In this report, we present part of the work carried out at our institute or in collaboration with external groups. We first focus on the magnetic order and the structural distortion observed in SrFe_2As_2 at atmospheric pressure and the connection between both phenomena. We then show that applying pressure leads to the suppression of the magnetostructural transition and the onset of superconductivity. The same occurs upon substituting Co on the Fe site. Both results allow a critical assessment of the similarity between Fe pnictides and cuprates. Finally, we provide evidence for re-entrant superconductivity in EuFe_2As_2 , which is the first example for a strong interaction between superconductivity within the FeAs layers and $4f$ magnetism on an interlayer site. All the experimental results are discussed in close connection to results of density functional based band-structure calculations.

Further details as well as the description of the experimental methods can be found in the original publications, Ref. 10 and 12-19.

Magnetic and structural properties of SrFe_2As_2

In a first step, we addressed the nature of the transition observed at $T_0 = 205 \text{ K}$ [10]. In the 1111 compounds it is presently believed that the AF-ordering of Fe moments occurs $\approx 20 \text{ K}$ below the

transition from the tetragonal to the orthorhombic structure, thus both transition being distinct. The first report on BaFe_2As_2 suggested the two transition to be closer and of second order. Thanks to an excellent polycrystalline sample, as evidence by a record residual resistivity ratio of 32 and an extremely sharp transition with a width of less than 0.5 K , we could demonstrate that in SrFe_2As_2 both AF ordering and structural distortion occur strictly simultaneously and in a first-order transition. This is evidenced by the anomalies in $\rho(T)$, $\chi(T)$, and $C(T)$ shown in Fig. 2(a). The former two present sharp step-like drops, and the latter one a sharp peak, the details of which (not shown) reveal a thermal arrest as expected for a first-order transition [10]. It is meanwhile consensus that the picture we proposed for SrFe_2As_2 also applies for the other $A\text{Fe}_2\text{As}_2$ systems with $A = \text{Ca}, \text{Ba},$ and Eu .

In order to obtain deeper insight regarding the relation between AF order and structural transition, we looked at the temperature dependence of both order parameters. The lattice distortion was investigated by means of x-ray powder diffraction. In Fig. 2(b) we show the abrupt splitting of the 220 tetragonal peak into the 400 and 040 peak of the orthorhombic structure. We used these data to determine the order parameter δ of the structural transition, defined from the orthorhombic lattice parameters by $a_{\text{OT}} = a_{\text{TT}}\sqrt{2(1+\delta)}$ and $b_{\text{OT}} = a_{\text{TT}}\sqrt{2(1-\delta)}$. The temperature dependence of δ normalized to its low- T value $\delta_0 = 0.56 \times 10^{-2}$ is shown in Fig. 3.

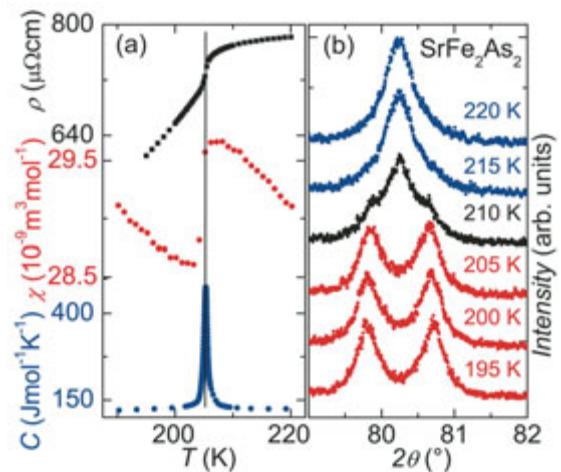


Fig. 2: (a) Electrical resistivity, magnetic susceptibility, and specific heat in SrFe_2As_2 near the first-order transition at $T_0 = 205 \text{ K}$. (b) Splitting of the 220 tetragonal peak into the 400 and 040 peaks of the orthorhombic structure below T_0 .

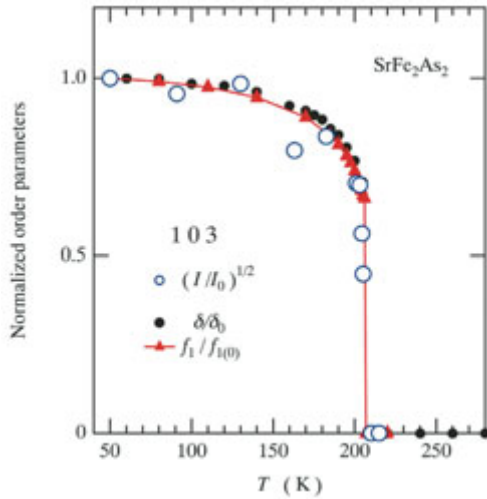


Fig. 3: Temperature dependence of the 103 magnetic reflection intensity normalized to that at 1.5 K, plotted as $\sqrt{I/I_0}$ (open circles), which is proportional to the size of the ordered moment. Closed circles and triangles correspond to the temperature dependence of normalized lattice distortion δ/δ_0 and the muon precession frequency f_1 , respectively, of SrFe_2As_2 .

Precise information on the evolution of the magnetic order parameter was obtained from muon spin relaxation (μSR) experiments. μSR is a well-established method for revealing and studying magnetic order. It probes the local field induced at the site(s) of the muon by slowly fluctuating or ordered nearby magnetic moments. For temperatures above 205 K we observe only a slow decay of the muon polarization, as expected for a nonmagnetic material. Below 205 K, well defined and strong oscillations appear in the time dependence of the muon polarization evidencing a precession of the muon in an internal field. The precession frequencies observed in our SrFe_2As_2 sample are much sharper than those observed in the 1111 compounds, confirming the higher homogeneity and quality of our SrFe_2As_2 sample in particular and of the 122 compounds in general. The precession frequency is proportional to the size of the ordered Fe moments, which corresponds to the magnetic order parameter. In Fig. 3 we plotted the temperature dependence of the precession frequency f_1 (corresponding to the largest contribution in the muon signal) again normalized to its low- T value. The comparison shows that the T -dependence of the magnetic order parameter and that of the structural order parameters are identical within experimental accuracy, confirming the intimate relation between both ordering phenomena. As pointed out by *P.*

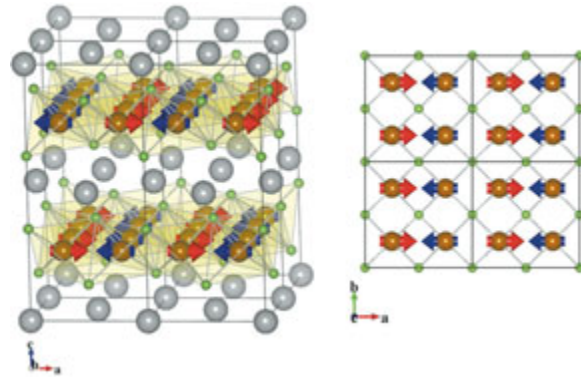


Fig. 4: Crystal and magnetic structure of SrFe_2As_2 in the ground state. The AFM coupling is along the a direction having the longer Fe-Fe distance, corresponding to $\mathbf{q} = (1\ 0\ 1)$. The Fe magnetic moment lies within the Fe plane and is aligned parallel to the a axis.

Thalmeier, such a linear relation between magnetic and structural order parameter contrasts with the quadratic dependence expected within standard Landau theories for phase transitions.

Additionally, we used neutron powder diffraction to determine important details in the magnetic structure of SrFe_2As_2 . While previous experiments already confirmed that the AFe_2As_2 systems present the same in-plane AF columnar ordering as in the 1111 systems, it was not clear along which of the orthorhombic directions the Fe moments order ferromagnetically and along which directions they order antiferromagnetically. By precise measurements and a careful analysis of the data we could conclusively demonstrate that the antiferromagnetic order occurs along the large Fe-Fe distance while the ferromagnetic order occurs along the shorter Fe-Fe distance. Moreover, we could also unambiguously demonstrate that the Fe moments are oriented parallel to the long Fe-Fe distance, i.e. the AF direction (see Fig. 4). The size of the ordered moment, $1.01(3)\ \mu_B$ turned out to be much larger than that proposed for the 1111 systems, although the values of the transferred fields observed in Mößbauer spectroscopy and μSR experiments are not too different. This suggests some problems with the neutron data on the 1111 systems likely related to the quality of the samples. We added in Fig. 3 the temperature dependence of the size of the ordered moment as deduced from our neutron diffraction data. It also follows nicely the temperature dependence observed in the μSR and x-ray diffraction experiments, despite a larger scattering due to weaker intensity.

Pressure studies on SrFe₂As₂

Superconductivity with T_c above 10 K was observed in the Fe pnictides originally only upon doping, similar to the cuprates. Since we expected the Fe-pnictides to be much more itinerant and much less strongly correlated than the cuprates we very soon asked ourselves whether it is possible to induce superconductivity only by applying pressure, without doping, as can be done e.g. in Kondo lattice systems. We therefore started an investigation of the effect of pressure on the temperature dependent resistivity.

First we focus on the pressure dependence of the magnetostructural transition at T_0 . On increasing pressure the feature in the resistivity $\rho(T)$ at T_0 becomes broader but remains well defined up to the highest pressure of our experiment. There is no qualitatively different behavior between the polycrystalline and the single crystalline material. In order to get additional information on the effect of pressure on this transition, we carried out temperature-dependent high-pressure x-ray diffraction studies for pressures of up to 4.4 GPa and temperatures down to 140 K. We performed two nearly isothermal and isobaric runs, respectively. For each run we could observe a clear phase transition from the tetragonal to the orthorhombic phase with decreasing temperature or a suppression of the distortion with increasing pressure. Comparing the phase boundary constructed from the x-ray diffraction and the electrical-resistivity data for both poly- and single-crystalline samples, we find excellent agreement between all measurements (Fig. 5). We clearly observe an orthorhombic phase at low temperatures for pressures below 3.8 GPa

To obtain a better understanding of the microscopic nature, we performed band structure calculations. At ambient pressure, the occurrence of the orthorhombic phase is intimately linked to antiferromagnetism. According to our electronic structure calculations, this intimate connection between the antiferromagnetic order and the orthorhombic distortion is preserved under pressure. Simulating hydrostatic pressure in our calculations, we find that the magnetic instability disappears at about 10% volume reduction, corresponding to a critical pressure of slightly more than 10 GPa. This value should be considered as a rough upper estimate since it suffers from the known LDA overestimate of magnetism in this class of compounds. In con-

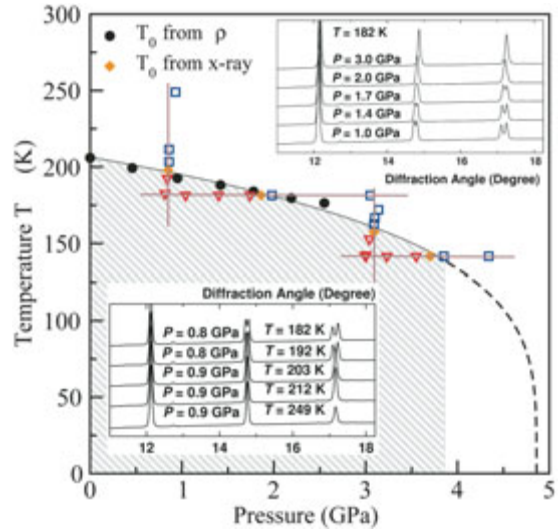


Fig. 5: Temperature-pressure phase diagram of SrFe₂As₂ with T_0 values from the evaluation of resistivity data (polycrystal-filled circles; single crystal-stars) and x-ray diffraction data (filled diamonds). The data points for the latter measurements are shown as open squares and triangles for the tetragonal and the orthorhombic phases, respectively. The approximately isobaric and isothermal runs are guided by horizontal and vertical lines. Exemplary x-ray diffraction patterns are presented in the upper and lower insets. The splitting of the reflections at about 15° and 17° indicates the structural transition. The measured region for the orthorhombic (magnetic) phase is shaded in gray. The dashed line is an extrapolation of the phase boundary down to zero temperature.

trast to CaFe₂As₂, where our calculations indicate the tetragonal collapsed phase similar to that in Ref. 22, we find no such transition for AFe₂As₂ ($A = \text{Sr, Ba, Eu}$) for pressures below 4 GPa. This suggests that the c/a collapse of the tetragonal phase is without general relevance for the superconductivity of the AFe₂As₂ compound family.

We now turn to the anomalies which emerged in $\rho(T)$ at low T above 2.5 GPa. At 2.55 GPa a sharp decrease in resistivity shows up below 40 K in the data of the polycrystalline sample. In the single crystal a similar reduction is observed at a slightly higher pressure ($p = 2.88$ GPa) and at somewhat lower temperature (see Fig. 6). However, we do not observe zero resistance at any pressure investigated in this study. The transition temperature T_c is in the same range where electron-doped SrFe₂As₂ becomes superconducting, giving a hint at a superconducting origin for the reduced resistance below T_c . To further elucidate the nature of the transition, we applied a magnetic field. The observed shift of T_c with magnetic field is typical for the superconducting iron arsenide compounds. From these in-

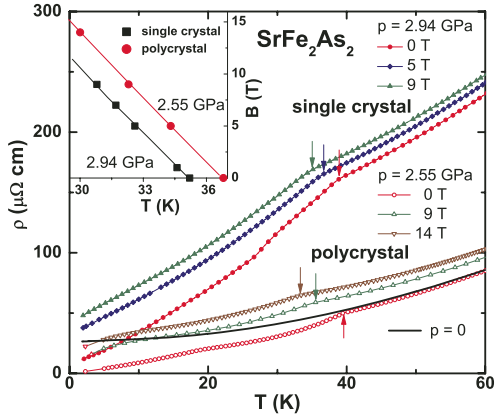


Fig. 6: Electrical resistivity of SrFe_2As_2 at $p = 2.55$ GPa (polycrystal, open symbols) and at $p = 2.94$ GPa (single crystal, solid symbols) in different applied magnetic fields. The solid line represents the ambient-pressure data for the polycrystalline sample as a reference. The arrows indicate T_c . Inset: B - T diagram compiled from the resistivity data.

indications we speculate that the observed drop in the electrical resistivity indicates indeed the emergence of a superconducting phase in SrFe_2As_2 , which has meanwhile been confirmed by other groups (Ref. 23, 24, and 25). The observation of a finite resistance well below T_c is attributed to the sensitivity of the Fe pnictides to strain. We also suspect that we are just below the critical point.

Co-substitution on the Fe site in SrFe_2As_2

One way to get insight into the superconducting mechanism is a doping experiment on the Fe site. Doping on sites in-between the Fe-As layers, either on the R or the O site in $R\text{FeAsO}$ systems or on the A site in $A\text{Fe}_2\text{As}_2$ compounds corresponds, both in a localized and in an itinerant model, to a simple charge doping and is therefore not suitable for discriminating between both models. In an itinerant model, within a simple rigid-band approach, the substitution of a small amount of Fe by another $3d$ element is expected to be similar to indirect doping via interlayer sites since only the total count of electrons is relevant. In a picture with localized $3d$ electrons, doping on the Fe site should lead to a drastically different behavior since correlations in the $3d$ layers are directly affected.

Therefore, we investigated the properties of the solid solution $\text{SrFe}_{2-x}\text{Co}_x\text{As}_2$. Co substitution leads to a rapid decrease of T_0 , followed by the onset of bulk superconductivity in the concentration range $0.2 \leq x \leq 0.4$. The maximum T_c of ≈ 20 K is

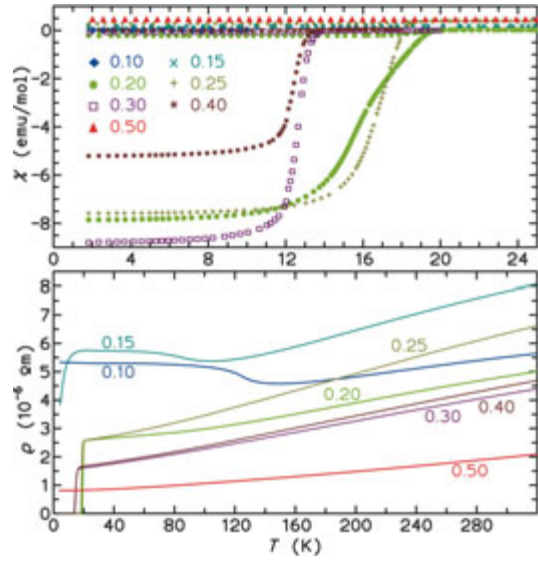


Fig. 7: Top: magnetic susceptibility $\chi(T)$ of $\text{SrFe}_{2-x}\text{Co}_x\text{As}_2$ samples in a nominal field of $\mu_0H = 2$ mT. Bottom: electrical resistivity of the same samples.

achieved for $x \approx 0.2$. The temperature dependence of the resistivity $\rho(T)$ (Fig. 7, bottom) at high T is generally metallic. $\rho(300$ K) decreases gradually with electron doping from $8 \mu\Omega\text{m}$ for $x = 0.15$ to $2 \mu\Omega\text{m}$ for $x = 0.5$, as also observed for potassium substituted samples [11]. For $x = 0.1$ a step-like increase of $\rho(T)$ is observed below ≈ 130 K. This step shifts to ≈ 90 K for $x = 0.15$. This anomaly can be assigned to the AF ordering and the related lattice distortion observed at $T_0 \approx 205$ K in SrFe_2As_2 [10, 25]. Thus, Co substitution (electron doping) leads to the suppression of the AF order in a similar way as reported for K substitution (hole doping) [4]. For $x = 0.2$ no such anomaly is seen and the compound exhibits a superconducting transition at 19.4 K. In the $x = 0.2$ – 0.4 samples the magnetic susceptibility in a nominal field $\mu_0H = 2$ mT (Fig. 7, top) displays strong diamagnetic signals in zero-field cooling due to superconducting transitions with onset temperatures T_c^{mag} up to 19.2 K. The compounds with $x = 0.1$ and $x = 0.5$ show no traces of superconductivity for $T \geq 1.8$ K. The specific heat shows a rounded anomaly at T_c as determined from resistivity and susceptibility confirming the bulk nature of superconductivity in $\text{SrFe}_{2-x}\text{Co}_x\text{As}_2$.

The appearance of superconductivity due to in-plane Co doping as such, provides strong evidence that an analogy with the high- T_c cuprates is not justified. We thus performed band structure calculations and discussed the electronic structure in

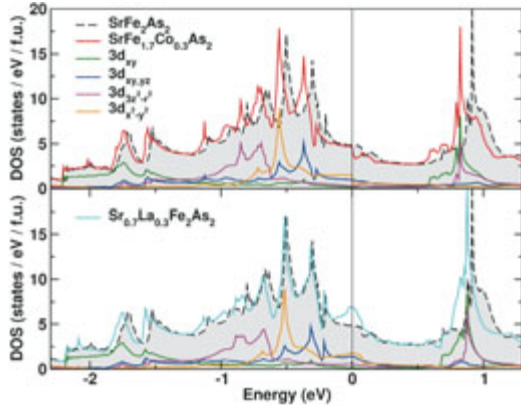


Fig. 8: Non magnetic total and Fe orbital resolved DOS from a VCA calculation for a 15% electron doping on the Fe site in SrFe_2As_2 . Upon electron doping, the DOS remains unchanged and displays a rigid-band-like behavior. Bottom: Non-magnetic total and Fe orbital resolved DOS for a 30% electron doping on the Sr site in SrFe_2As_2 . Addition of electrons changes the shape of the DOS close to ϵ_F drastically. A pronounced peak starts to appear close to ϵ_F which tends to destabilize the system. The changes in the total DOS for various doping concentrations are shown in the right panel.

view of our experimental results. The electron doping upon Co substitution on the iron site results in a reduction of the density of states (DOS) at the Fermi level ϵ_F (see Fig. 8) and for a critical Co concentration to a suppression of the magnetic order. In contrast, electron doping on the Sr site by La substitution leads to an increase of the DOS at ϵ_F (see Fig. 8). From consistency of our itinerant approach with the experimental results we conclude that an itinerant picture is more appropriate for these layered Fe-As systems than a localized description.

Recently, we have reported on further substitutions on the Fe site in SrFe_2As_2 . While electron doping by Ni substitution likewise to Co generates superconductivity, a hole doping with Mn does not lead to a suppression of the AF phase and therefore not to superconducting alloys [19].

Evidence for re-entrant superconductivity in EuFe_2As_2

In contrast to the $A\text{Fe}_2\text{As}_2$ ($A = \text{Ca}, \text{Sr}, \text{Ba}$) compounds where only the iron possesses a magnetic moment, in EuFe_2As_2 a large additional magnetic moment of $7\mu_B$ is carried by Eu which is in the $2+$ state. Like the ($A = \text{Ca}, \text{Sr}, \text{Ba}$) members of the $A\text{Fe}_2\text{As}_2$ family, EuFe_2As_2 exhibits a SDW transition around $T_0 \approx 190$ K related to the Fe_2As_2 layers, but additionally at $T_N \approx 20$ K the magnetic mo-

ments of the localized Eu^{2+} moments order antiferromagnetically [12,26-28]. EuFe_2As_2 has structural properties very similar to SrFe_2As_2 , the unit-cell volume is only 3% smaller, and the value of T_0 are comparable. Furthermore, aside from the Eu 4f part, the electronic DOS of EuFe_2As_2 is almost identical to the DOS of SrFe_2As_2 (see Fig. 9). Therefore, SrFe_2As_2 can be considered as a homologue compound of EuFe_2As_2 without 4f magnetism. Provided that the two different kinds of magnetic ordering phenomena are reasonably well decoupled, the results of previous doping and pressure studies on SrFe_2As_2 [15,16,22] would suggest the appearance of a superconducting phase on doping and/or at high pressure in EuFe_2As_2 too.

Figure 10 shows the electrical resistivity, $\rho(T)$, of EuFe_2As_2 for different applied pressures. In the whole investigated pressure range the resistivity decreases continuously on decreasing temperature, with the exception of a clear anomaly indicating SDW type of magnetic transition at T_0 at low pressures. With increasing pressure the peak broadens. At $p = 2.3$ GPa only a change of slope in $\rho(T)$ remains. At higher pressures this anomaly can no longer be detected unambiguously. At low temperature a second anomaly appears around $T_N \approx 20$ K indicating the magnetic ordering of the Eu^{2+} moment. T_N seems to be nearly pressure independent. At $p = 2.03$ GPa a sharp drop of the resistivity appears around $T_c = 29.5$ K. With increasing pressure this drop becomes even sharper and more pronounced, while its position does not change. We ascribe this feature in the resistivity to the on-

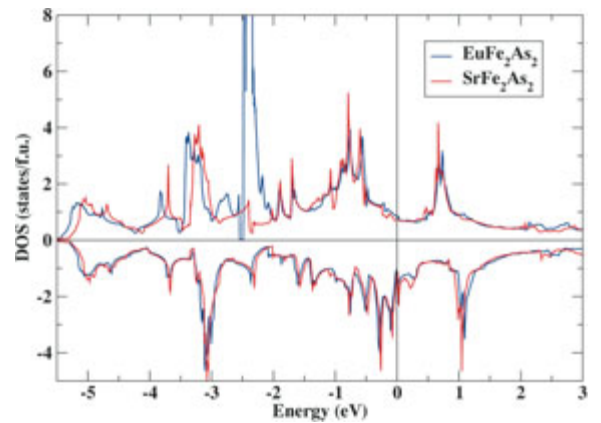


Fig. 9: Comparison of the total DOS for EuFe_2As_2 (LSDA+U, with ferromagnetic interaction between the Eu and Fe spins) and SrFe_2As_2 (LSDA). The experimental lattice was used for both compounds. The large peak for the spin-up states at -2.2 eV arises from the fully filled Eu 4f states. The unfilled Eu 4f states are at 9.5 eV above the Fermi level.

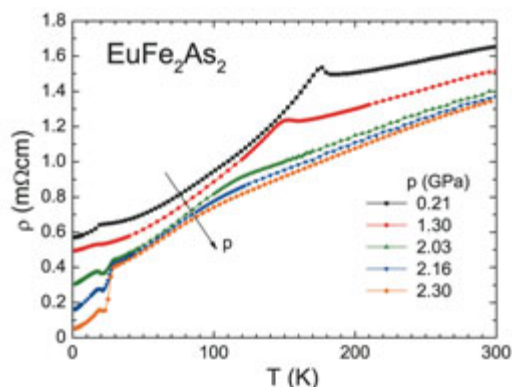


Fig. 10: Electrical resistivity vs. temperature for different applied pressures for single crystalline EuFe_2As_2 .

set of superconductivity. The complete formation of the superconducting state is interrupted by the ordering of the Eu^{2+} sublattice at $T_N < T_c$. The ordering of the Eu^{2+} causes an initial increase of $\rho(T)$ followed by a maximum on lowering the temperature. This behavior of $\rho(T)$ is reminiscent of re-entrant superconductivity which has first been reported in the Chevrel phase HoMo_6S_8 [30] and later in the rare-earth nickel borocarbides (e.g. $\text{HoNi}_2\text{B}_2\text{C}$) [30].

Such a reentrant superconductivity as well as the suspected suppression of the superconducting state by the antiferromagnetic state at higher field has not been observed in the doped RFeAsO compounds, likely because there T_c is much larger than T_N of the $4f$ moments. This makes EuFe_2As_2 unique among the layered FeAs systems.

Summary

With our experiments and calculations on pure and doped SrFe_2As_2 and EuFe_2As_2 , we contribute to reveal the intriguing properties of the Fe-As systems and to a preliminary understanding of these properties. We demonstrate an intimate connection between the magnetic order and the structural distortion in the AFe_2As_2 compounds. We showed that applying pressure on the undoped compounds leads to a suppression of the magnetostructural transition and to the appearance of superconductivity. The same effect can be obtained by doping in the Fe-As plane instead of doping in between the layers. These results as well as the excellent agreement with our LDA based calculations evidence that these systems are much more itinerant than the cuprates.

References

- [1] Y. Kamihara, T. Watanabe, M. Hirano, and H. Hosono, *J. Am. Chem. Soc.* **130** (2008) 3296.
- [2] Z. A. Ren *et al.*, *Chin. Phys. Lett.* **25** (2008) 2215.
- [3] K. Sasmal *et al.*, *Phys. Rev. Lett.* **101** (2008) 107007.
- [4] G. F. Chen *et al.*, *Chin. Phys. Lett.* **25** (2008) 3403.
- [5] M. Rotter, M. Tegel, and D. Johrendt, *Phys. Rev. Lett.* **101** (2008) 107006.
- [6] X. C. Wang *et al.*, (2008), arXiv:0806.4688.
- [7] Y. Mizuguchi *et al.*, *Appl. Phys. Lett.* **93** (2008) 152505.
- [8] G. Wu, *et al.*, *J. Phys.: Condens. Matter* **21** (2009) 142203.
- [9] F. Ronning *et al.*, *J. Phys.: Condens. Matter* **20** (2008) 322201.
- [10] C. Krellner *et al.*, *Phys. Rev. B* **78** (2008) 100504(R).
- [11] M. Rotter *et al.*, *Phys. Rev. B* **78** (2008) R020503.
- [12] H. S. Jeevan *et al.*, *Phys. Rev. B* **78** (2008) 052501.
- [13] A. Jesche *et al.*, *Phys. Rev. B* **78** (2008) 180504(R).
- [14] H. S. Jeevan *et al.*, *Phys. Rev. B* **78** (2008) 092406.
- [15] A. Leithe-Jasper *et al.*, *Phys. Rev. Lett.* **101** (2008) 207004.
- [16] M. Kumar *et al.*, *Phys. Rev. B* **78** (2008) 184516.
- [17] C. F. Miclea *et al.*, (2008) arXiv:0808.2026.
- [18] K. Kaneko *et al.*, *Phys. Rev. B* **78** (2008) 212502.
- [19] D. Kasinathan *et al.*, *New. J. Phys.* **11** (2009) 025023.
- [20] G. F. Chen *et al.*, *Phys. Rev. B* **78** (2008) 224512.
- [21] A. Kreyssig *et al.*, *Phys. Rev. B* **78** (2008) 184517.
- [22] P. L. Alireza *et al.*, *J. Phys.: Condens. Matter* **21** (2008) 012208.
- [23] M. S. Torikachvili *et al.*, *Phys. Rev. B* **78** (2008) 104527.
- [24] K. Igawa *et al.*, *J. Phys. Soc. Jpn.* **78** (2009) 025001.
- [25] M. Tegel *et al.*, *J. Phys.: Condens. Matter* **20** (2008) 452201.
- [26] H. Raffius *et al.*, *J. Phys. Chem. Solids* **54** (1993) 135.
- [27] Z. Ren *et al.*, *Phys. Rev. B* **78** (2008) 052501.
- [28] S. Jiang *et al.*, *New. J. Phys.* **11** (2009) 025007.
- [29] M. Ishikawa and Ø. Fischer, *Solid State Comm.* **23** (1977) 37.
- [30] H. Eisaki *et al.*, *Phys. Rev. B* **50** (1994) 647.

¹Laboratory for Muon-Spin Spectroscopy, Paul-Scherrer-Institute, 5232 Villigen, Switzerland

²I. Physikalisches Institut, Georg-August-Universität Göttingen, 37077 Göttingen, Germany

³ESRF, BP 220, 38043 Grenoble Cedex 9, France

⁴Hahn-Meitner-Institute, 14109 Berlin, Germany

⁵Department of Physics, Indian Institute of Technology, Kampur 208016, India

⁶Permanent address: Advanced Science Research Center, Japan Atomic Energy Agency, Tokai, Ibaraki 319-1195, Japan

⁷IFP, Technische Universität Dresden, 01069 Dresden, Germany